A vortex-dynamical scaling theory for flickering buoyant diffusion flames

Xi Xia[1] **and Peng Zhang**[1, †]

[1]Department of Mechanical Engineering.
The Hong Kong Polytechnic University, Hung Hom, Hong Kong

The flickering of buoyant diffusion flames is associated with the periodic shedding of toroidal vortices that are formed under gravity-induced shearing at the flame surface. Numerous experimental investigations have confirmed the scaling, $f \propto D^{-1/2}$, where f is the flickering frequency and D is the diameter of the fuel inlet. However, the connection between the toroidal vortex dynamics and the scaling has not been clearly understood. By incorporating the finding of Gharib *et al.* (1998) that the detachment of a continuously growing vortex ring is inevitable and can be dictated by a universal constant that is essentially a non-dimensional circulation of the vortex, we theoretically established the connection between the periodicity of the toroidal vortices and the flickering of a buoyant diffusion flame with small Froude number. The scaling theory for flickering frequency was validated by the existing experimental data of pool flames and jet diffusion flames.

Key words: buoyant diffusion flames, flame instability, flickering frequency, toroidal vortex, vortex formation/detachment.

---

1. Introduction

Diffusion flames are ubiquitous in domestic and industrial applications that have been shaping the human civilization, including energy production, propulsion, and fire protection. Diffusion flames, if being away from extinction, are controlled by the convection and diffusion of species in the flow field where the flame is embedded, and are less affected by chemical reactions, which usually happen within a short period of time and inside a limited space (Burke & Schumann 1928; Liñán *et al.* 2015). In practice, diffusion flames tend to become unstable under the effect of buoyancy (Chen *et al.* 1989; Cox 1995; Coats 1996; Lingens *et al.* 1996; Tieszen *et al.* 1996; Malalasekera *et al.* 1996; Joulain 1998; Jiang & Luo 2000; Tieszen 2001; Liñán *et al.* 2005; Carpio *et al.* 2012; Zhu *et al.* 2018). A prominent phenomenon related to the stability of a buoyant diffusion flame is the flame flickering (Chamberlin & Rose 1948) or puffing, which describes the vibratory motion of the luminous flame, especially on its the upper part, and has been a constant subject of interest for several decades.

Early studies (McCamy 1956; Byram & Nelson 1970; Portscht 1975; Sibulkin & Hansen 1975; Detriche & Lanore 1980; Zukoski *et al.* 1985) experimentally found that flame flickering is a periodic phenomenon. The frequency associated with the periodicity, termed flickering frequency f in this context, is related to the fuel inlet diameter D as $f \propto D^{-1/2}$

† Email address for correspondence: pengzhang.zhang@polyu.edu.hk
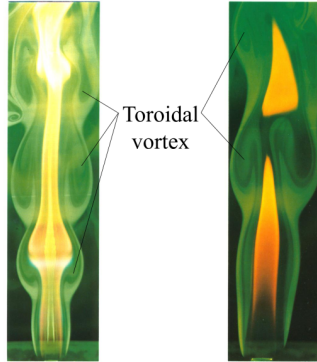
FIGURE 1. Flow visualizations of laminar jet diffusion flames (Chen *et al.* 1989) show the synchronization between the flame structures and the toroidal vortices.

with a proportionality factor of around 1.5 given by Trefethen & Panton (1990) and Cetegen & Ahmed (1993). Slightly different values of the factor have been reported by others (Byram & Nelson 1970; Detriche & Lanore 1980; Malalasekera *et al.* 1996; Joulain 1998). Based on dimensional analysis, Byram & Nelson (1970) derived $f \propto (g/D)^{1/2}$, where g is the gravitational acceleration constant. This scaling law is equivalent to the Strouhal-Froude number correlation, $St \propto Fr^{-1/2}$, by Hamins *et al.* (1992) and Malalasekera *et al.* (1996). The same scaling law was reproduced by Bejan (1991) with the use of buckling theory of inviscid streams. Cetegen & Ahmed (1993) extended the scaling law to account for the initial fuel momentum of buoyant jet diffusion flames by including the Richardson number.

The previous investigations point to a striking feature of flickering buoyant diffusion flames that the flickering is not due to the alternate extinction and re-ignition but a fluid-dynamical phenomenon. Buckmaster & Peters (1988) performed a linear stability analysis to an infinite candle model and attributed the flickering to Kelvin-Helmholtz instability. Chen and Roquemore (Chen & Roquemore 1986; Roquemore *et al.* 1987; Chen *et al.* 1989) together with coworkers presented the flow visualizations of laminar jet diffusion flames and identified two different types of vortices — the small vortices (inside of the luminous flame) developed due to the instability of the jet and the large toroidal vortices (outside of the flame) caused by the buoyancy-induced Kelvin-Helmholtz instability. According to Chen *et al.* (1989), the toroidal vortices are responsible for the detachment of the flame puff, which is also known as the flame pinch-off (Davis *et al.* 1990; Carpio *et al.* 2012), and the "pairing" and "merging" of the flame bulge, rendering the periodic flame flickering as illustrated in figure 1. This was also confirmed by the numerical simulation of Katta & Roquemore (1993). Cetegen & Ahmed (1993) further substantiated this view by predicting the flickering frequency based on the convective time scale associated with a toroidal vortex. Subsequently, numerous experimental and numerical investigations have been conducted to study the dynamics of the toroidal vortices and their interaction with flame (Katta *et al.* 1994; Mell *et al.* 1996; Ghoniem *et al.* 1996; Cetegen 1997; Maxworthy 1999; Albers & Agrawal 1999; Jiang & Luo 2000; Tieszen 2001; Kolhe & Agrawal 2007). It is quite clear now that flickering is primarily caused by buoyant flow instability and the toroidal vortices, at least at sufficiently small Reynolds numbers.

To this day, the jigsaw puzzle of the flame flickering has almost been completed, left with only a few unsolved pieces, one of which is the connection between the dynamics of toroidal vortices and the flame flickering frequency. The first and, thus far, probably

the only theoretical attempt was made by Cetegen & Ahmed (1993), who applied the Bernoulli equation to estimate the flow velocity of the flame sheet and then derived a formula of flickering frequency. However, their formula depends on an implicit assumption that the height of the flame puff risen during a period is proportional to the flame inlet dimension, which has not been justified to date. In the current study, the germane and critical problem is to mathematically elucidate how the vortex dynamics, including the generation of vorticity, the roll-up of the toroidal vortex, and the vortex detachment, can be integrated into a theory that quantitatively determines the flame flickering. To this end, a primary task of the current study is to establish a unified vortex-dynamical scaling theory to predict the frequency of various pool flames and jet diffusion flames reported in the literature.

2. Vortex sheet formation of flickering buoyant diffusion flames

As stated above, the essence of the flickering flame lies in the dynamics of the toroidal vortices. The first question to ask is how the toroidal vortex forms. In vortex dynamics, the formation and evolution of toroidal vortex, formally known as the "vortex ring", have been studied extensively (Maxworthy 1972, 1977; Saffman 1978; Didden 1979; Glezer 1988; Shariff & Leonard 1992; Gharib *et al.* 1998). Physically, the appearance of a vortex ring may be considered as the outcome of the growing and rolling-up of a cylindrical-shaped vortex sheet. A well-known example is the starting vortex jet (Didden 1979; Nitsche & Krasny 1994; Gharib *et al.* 1998; Mohseni & Gharib 1998), where the vortex sheet is continuously supplied by pushing a fluid slug out of a circular jet nozzle to form a cylindrical shear layer. From this perspective, the toroidal vortex of a diffusion flame should not be fundamentally different and its formation must involve a growing vortex sheet.

A schematic of vortex sheet in a laminar diffusion flame is shown in figure 2. The vorticity growth inside the vortex sheet is governed by the vorticity transport equation,

$$\frac{\mathrm{D}\boldsymbol{\omega}}{\mathrm{D}t} = (\boldsymbol{\omega} \cdot \nabla)\boldsymbol{u} - \boldsymbol{\omega}(\nabla \cdot \boldsymbol{u}) + \frac{1}{\rho^2}(\nabla\rho \times \nabla p) + \frac{\rho_A}{\rho^2}(\nabla\rho \times \boldsymbol{g}) + \nu\nabla^2\boldsymbol{\omega}, \qquad (2.1)$$

where $\boldsymbol{u}$ and $\boldsymbol{\omega}$ are the velocity and vorticity vectors, ρ the local density, and p the gauge pressure, $\boldsymbol{g}$ the gravitational acceleration vector, ν the kinematic viscosity, and ρ_A the gas density of the ambient environment. On the right-hand side of (2.1), the first vortex tilting/stretching term vanishes for either two-dimensional flows or axisymmetric flows without swirling, the second dilatation term vanishes for incompressible flows, and the fifth diffusion term describes the redistribution of vorticity and thus is not a source of vorticity production. Vorticity generation are attributed to the third baroclinic term and the fourth gravitational term, both of which entail the presence of variable density. In this case, the growth of vortex sheet is caused by the flame-induced vorticity addition mechanisms, which differ from the vorticity flux supplied by the inflow of a jet.

To evaluate the formation of a flame-induced vortex sheet (or viscous shear layer) and its roll-up into a toroidal vortex, we focus on the circulation (Γ) of a control mass, defined by

$$\Gamma = \oint_{\partial A} \boldsymbol{u} \cdot \mathrm{d}\boldsymbol{s}. \qquad (2.2)$$

As illustrated in figure 2, the dashed box ∂A is a material contour around the vortex sheet segment between s_{v1} and s_{v2}, and A is the area encircled by the contour so A is a control mass; $\mathrm{d}\boldsymbol{s}$ represents a material line element along ∂A. The vorticity vector has only one azimuthal component as $\boldsymbol{\omega} = \omega\hat{\boldsymbol{\theta}}$ under the assumption of axisymmetric flow without
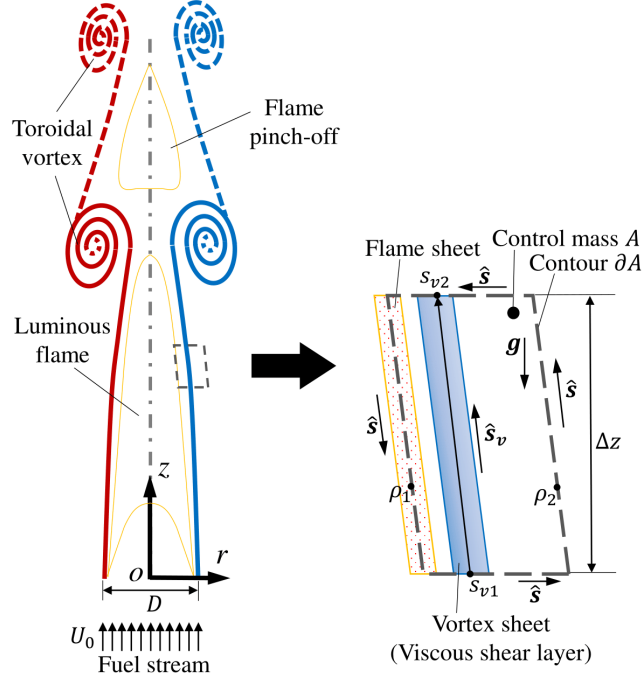
FIGURE 2. Schematic of the vortex sheet for the growth of a toroidal vortex in an axisymmetric laminar diffusion flame. Note that the zero thickness of flame and vortex sheets is exaggerated for illustration.

swirling (the axial vorticity is important in swirling flames as studied by Klimenko & Williams (2013) and Yu & Zhang (2017*a*,*b*)). Applying the divergence theorem to (2.2) yields $\Gamma = \iint \omega \mathrm{d}A$, meaning Γ is a measure for the total vorticity inside A.

The rate of total change of Γ can be derived from (2.2) as

$$\frac{\mathrm{d}\Gamma}{\mathrm{d}t} = \oint_{\partial A} \frac{\mathrm{D}\boldsymbol{u}}{\mathrm{D}t} \cdot \mathrm{d}\boldsymbol{s} + \oint_{\partial A} \boldsymbol{u} \cdot \frac{\mathrm{D}(\mathrm{d}\boldsymbol{s})}{\mathrm{D}t}. \tag{2.3}$$

According to the identity $\mathrm{D}(\mathrm{d}\boldsymbol{s})/\mathrm{D}t = \mathrm{d}\boldsymbol{u}$ (Wu *et al.* 2007), the second integral term of (2.3) vanishes as $\oint_{\partial A} \boldsymbol{u} \cdot \mathrm{d}\boldsymbol{u} = \oint_{\partial A} \mathrm{d}(\boldsymbol{u} \cdot \boldsymbol{u})/2 = 0$; the integrand $\mathrm{D}\boldsymbol{u}/\mathrm{D}t$ in the first integral term is given by the Navier-Stokes equation,

$$\frac{\mathrm{D}\boldsymbol{u}}{\mathrm{D}t} = -\frac{1}{\rho}[\nabla p + (\rho_A - \rho)\boldsymbol{g}] + \nu\nabla^2\boldsymbol{u}, \tag{2.4}$$

where the gauge pressure p is related to the absolute pressure p_{ab} as $\nabla p_{ab} = \nabla p + \rho_A \boldsymbol{g}$. Here, $\nu\nabla^2\boldsymbol{u}$ is the shear stress (per unit mass) and approaches zero outside the viscous shear layer, where the flow is effectively inviscid. This implies $\nu\nabla^2\boldsymbol{u} = \boldsymbol{0}$ on ∂A. $|\nabla p|/|(\rho_A - \rho)\boldsymbol{g}|$ physically represents a characteristic Froude number. For buoyancy-dominated flames, we adopt the small Froude number assumption ($Fr \ll 1$) so the pressure gradient is negligible compared with the gravity term in (2.4). With $\mathrm{d}\boldsymbol{s}$ expressed as $\hat{\boldsymbol{s}}\mathrm{d}s$, where $\hat{\boldsymbol{s}}$ is the unit tangential vector along the contour ∂A, equation (2.3) can be rewritten as

$$\frac{\mathrm{d}\Gamma}{\mathrm{d}t} = \oint_{\partial A} -\frac{\rho_A - \rho}{\rho}\boldsymbol{g} \cdot \hat{\boldsymbol{s}}\mathrm{d}s = \int_{s_{v1}}^{s_{v2}} \rho_A \left(\frac{1}{\rho_1} - \frac{1}{\rho_2}\right)(\hat{\boldsymbol{s}}_v \cdot \boldsymbol{g})\,\mathrm{d}s, \tag{2.5}$$

where $\hat{\boldsymbol{s}}_v$ is the unit tangential vector of the vortex sheet as shown in figure 2. Assuming

the gas density at either side of the vortex sheet is constant, which means $\rho_1(s) = \rho_f$ where ρ_f is the density of the gas at the flame sheet and $\rho_2(s) = \rho_A$, we have

$$\frac{\mathrm{d}\Gamma}{\mathrm{d}t} = \rho_A \left(\frac{1}{\rho_1} - \frac{1}{\rho_2} \right) \left(\int_{s_{v1}}^{s_{v2}} \mathrm{d}\hat{\boldsymbol{s}}_v \cdot \boldsymbol{g} \right) = -g\Delta z(r^* - 1), \tag{2.6}$$

where Δz is the vertical length of the vortex sheet associated with the control mass A, as shown in figure 2. The density ratio, $r^* = \rho_A/\rho_f$, is a measurable quantity for a given flame. For a rough estimation of r^*, assuming the flame is isobaric and following the ideal gas law, we have $r^* = \rho_A/\rho_f = T_f/T_A$, where T_A and T_f are the temperatures of the ambient air and the flame sheet, respectively. For common fuels burned in air, the flame temperature at normal atmospheric condition (1 atm, $T_A \approx 300$ K) varies in a wide range roughly between 1200 K and 2400 K, corresponding to the r^* range of $4 \sim 8$.

Equation (2.6) indicates an important feature of the buoyancy-induced vortex sheet that the generation rate of total vorticity (circulation) is independent of the geometric shape of the sheet, but only dictated by the vertical length of the sheet.

3. Formation of periodical toroidal vortices

It is evident from the flow visualization of Chen *et al.* (1989) and numerical simulation of Katta *et al.* (1994), among others, that the periodicity of the flame structures is strongly correlated with the toroidal vortices, which are rolled up from the buoyancy-induced vortex sheet. The study of unsteady diffusion flames by Cantwell *et al.* (1989) further illustrated the sequential evolution of an individual toroidal vortex and its coupling with the dynamics of the flame. Following these studies, we present the formation process of a toroidal vortex in figure 3 to illustrate the relation between the flickering flame and the periodic toroidal vortices. At $t = 0$, a previous toroidal vortex (marked by grey-dashed line) matures and detaches, leading to the generation of a new toroidal vortex near the base of the flame. This new vortex core together with its trailing vortex sheet (marked by blue-solid line) then grow and advect downstream under buoyancy. At $t = \tau$, where $\tau = 1/f$ is the period of flame flickering, the new toroidal vortex becomes fully developed and its circulation is defined as

$$\Gamma_{TV} = \Gamma_B(\tau) = \int_0^\tau \frac{\mathrm{d}\Gamma_B}{\mathrm{d}t}\mathrm{d}t, \tag{3.1}$$

where Γ_B is the total circulation of the moving control volume B (marked by the red-dashed box), which encloses the vortex core and its trailing vortex sheet.

The rate of change of Γ_B is given by

$$\frac{\mathrm{d}\Gamma_B}{\mathrm{d}t} = \frac{\mathrm{d}}{\mathrm{d}t} \int_B \mathrm{d}\Gamma = \frac{\mathrm{d}}{\mathrm{d}t} \int_0^{h(t)} \gamma_z(z,t)\mathrm{d}z, \tag{3.2}$$

where $\gamma_z(z,t) = \mathrm{d}\Gamma/\mathrm{d}t$. $h(t)$ is the height of the upper boundary of B, which rises following the convection of the toroidal vortex. Applying the Leibniz integral rule to (3.2), we have

$$\frac{\mathrm{d}\Gamma_B}{\mathrm{d}t} = \gamma_z(h(t),t)\frac{\mathrm{d}h(t)}{\mathrm{d}t} + \int_0^{h(t)} \frac{\partial \gamma_z(z,t)}{\partial t}\mathrm{d}z. \tag{3.3}$$

Considering the control mass $\mathcal{V}_B$ that instantaneously overlaps with the control volume B at time t, and applying (2.6) to $\mathcal{V}_B$, we can obtain the rate of change of the circulation
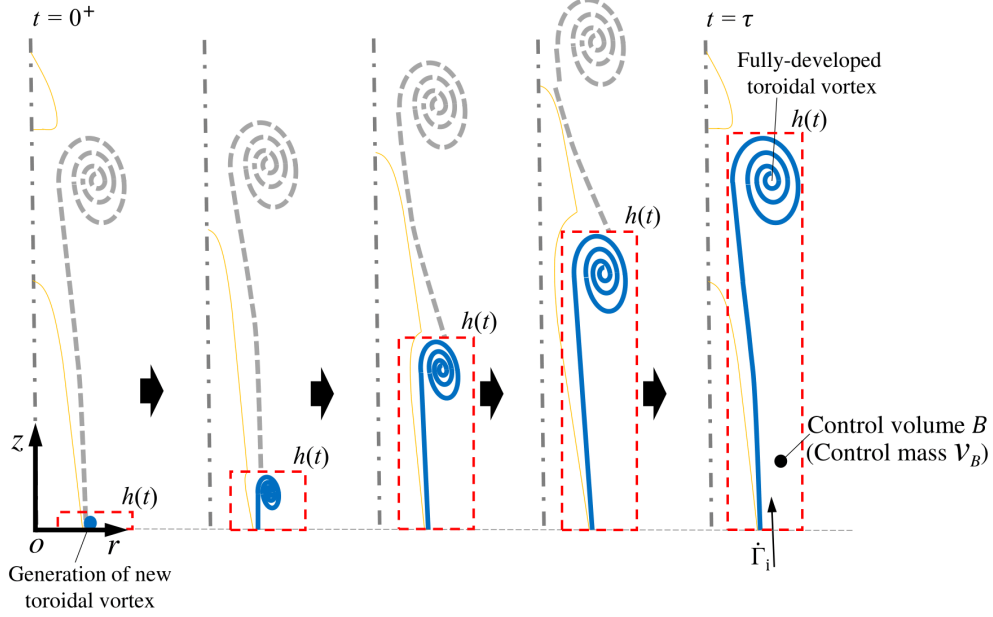
FIGURE 3. Schematic of the periodic formation process of a toroidal vortex. The vortex sheets associated with the formation of toroidal vortex are tracked by the blue-dashed lines.

in $\mathcal{V}_B$:

$$\frac{\mathrm{d}\Gamma_{\mathcal{V}_B}}{\mathrm{d}t} = -gh(t)(r^* - 1). \tag{3.4}$$

Further noting that $\Gamma_{\mathcal{V}_B} = \int_{\mathcal{V}_B} \gamma_z(z,t)\mathrm{d}z$, $\Gamma_{\mathcal{V}_B}$ can be also derived using the Reynolds transport theorem (Batchelor 1967) as

$$\begin{aligned}
\frac{\mathrm{d}\Gamma_{\mathcal{V}_B}}{\mathrm{d}t} &= \gamma_z(h(t),t) \left.\frac{\mathrm{d}z}{\mathrm{d}t}\right|_{z=h(t)} - \gamma_z(0,t) \left.\frac{\mathrm{d}z}{\mathrm{d}t}\right|_{z=0} + \int_0^{h(t)} \frac{\partial\gamma_z(z,t)}{\partial t}\mathrm{d}z \\
&= \gamma_z(h(t),t)\frac{\mathrm{d}h(t)}{\mathrm{d}t} - \gamma_z(0,t) \left.\frac{\mathrm{d}z}{\mathrm{d}t}\right|_{z=0} + \int_0^{h(t)} \frac{\partial\gamma_z(z,t)}{\partial t}\mathrm{d}z.
\end{aligned} \tag{3.5}$$

Comparing (3.3) and (3.5) and using (3.4), we obtain

$$\frac{\mathrm{d}\Gamma_B}{\mathrm{d}t} = -gh(t)(r^* - 1) + \dot{\Gamma}_{\mathrm{i}}(t), \tag{3.6}$$

where $\dot{\Gamma}_{\mathrm{i}}(t) = (\mathrm{d}\Gamma/\mathrm{d}t)|_{z=0}$ is the rate of circulation addition by the inflow, which enters the system through the lower boundary of B.

In the current study, $\dot{\Gamma}_{\mathrm{i}}(t)$ reflects the possible presence of an initial vortex sheet associated with the fuel stream at the fuel inlet, either from a jet or induced by evaporation of a pool flame. The fuel stream may be considered as a jet flow, the rate of circulation addition by which was given by Didden (1979) as

$$\dot{\Gamma}_{\mathrm{i}}(t) = -C_j U_0^2, \tag{3.7}$$

where U_0 is the initial jet velocity and C_j is a constant relating to the configuration and boundary condition of the jet exit. According to Krieg & Mohseni (2013), C_j is 0.5 for an ideal parallel-nozzle jet, but it could be inaccurate if the jet entrains a radial flow and causes additional circualtion generation. For example, the effective C_j for a converging

jet can be under-predicted by a factor of 3 (Krieg & Mohseni 2013). Consequently, we shall compare the results of $C_j = 0.5$ and $C_j = 1.5$ in the theoretical predictions.

Applying (3.6) and (3.7) to (3.1), we obtain

$$\Gamma_{TV} = -gH\tau(r^* - 1) - C_j U_0^2 \tau, \qquad (3.8)$$

where $H = \tau^{-1} \int_0^\tau h(t)\mathrm{d}t$ is the time-averaged height of the growing toroidal vortex. The integration of (3.8) is based on the assumption that the vortex sheet grows in a quasi-steady manner, given that the flame flickering period is so short that the densities of the gases across the vortex sheet remain approximately unchanged meanwhile.

In the current study, the two common types of diffusion flames are pool flames, where the fuel vapor enters the system from the evaporation of liquid pool, and jet flames, where the fuel stream is supplied via a gaseous jet. The initial fuel velocity U_0 is a given boundary condition for jet flames, whereas for pool flames it is an eigenvalue of the thermochemical-coupled equations (Yu & Zhang 2017a,b). The effect of fuel velocity on the flickering frequency of jet flames has been investigated by Hamins *et al.* (1992), Sato *et al.* (2000), and Fang *et al.* (2016), among others, which indicates the existence of two distinct regimes, namely momentum-driven and buoyancy-driven. Since buoyancy-driven flames have a characteristic velocity of $U = \sqrt{gD}$, the motion of the upper boundary of the toroidal vortex may be roughly estimated as $h(t) = C_h U t$ with C_h being a constant prefactor; so $H = C_h U \tau / 2$. With Γ_{TV} scaled by $-UD$, equation (3.8) can be written in the non-dimensional form as

$$\Gamma_{TV}^* = \frac{C_h}{2} Ri\tau^{*2} + C_j \sqrt{Fr}\tau^*, \qquad (3.9)$$

where $\tau^* = U_0\tau/D$. The Richardson number and the Froude number are defined as $Ri = (r^* - 1)gD/U_0^2$ and $Fr = U_0^2/gD$, respectively. It is noted that in theory equation (3.9) is only valid for buoyancy-driven flames that are characterized by $U_0 \ll U$, corresponding to $Fr \ll 1$ or $Ri \gg 1$.

In this study, we propose that the flame flickering is caused by the alternate formation and detachment of the toroidal vortices, the fundamental mechanism of which does not conflict with the Kelvin-Helmholtz instability proposed in the literature (Chen & Roquemore 1986; Buckmaster & Peters 1988; Chen *et al.* 1989). In fact, these mechanisms share two key similarities. First, both mechanisms are characterized by vortex roll-up. Second, they are caused by velocity shear, and are closely related to strength of the shear layer. The difference between them can be understood as spatial or temporal development of the instability. Specifically, a typical Kelvin-Helmholtz instability can be thought as a spatial one where multiple vortices roll up simultaneously along a uniform shear layer in space; whereas the periodical formation and detachment of vortices can be considered as a temporal instability where local growth of vortex sheet causes the vortices to develop in sequence. Thus, a series of fully-developed vortices together render the feature of the Kelvin-Helmholtz instability.

4. Theoretical predictions

The above analysis hitherto has addressed the formation and growth of a toroidal vortex, which leaves us another question: how does the toroidal vortex shed? The answer to a similar problem on vortex ring formation has been given by Gharib *et al.* (1998) and Mohseni & Gharib (1998), who pointed to the existence of a universal non-dimensional formation number, above which a vortex ring would be too strong to maintain growing and consequently detach from its vorticity-feeding shear layer. In other words, the forma-

tion number can be considered as a dimensionless measure of the upper limit of the total circulation of an attached vortex ring. This mechanism can be interpreted as a unified condition for the detachment of a rolled-up vortex ring. We hypothesize that the shedding of the current toroidal vortex is controlled by the same mechanism, because the strength of the vortex sheet is constantly growing under the buoyancy-induced vorticity generation, and will roll up into a vortex once the vortex sheet becomes sufficiently strong. However, this should be distinguished from the case of constant laminar flow through a nozzle, where the strength of the vortex sheet remains unchanged. As the result, the initial vortex sheet is too weak to roll up unless otherwise being disturbed or instability develops in the downstream. This explains why a continuous laminar jet generally does not have alternate formation and detachment of vortex rings.

From the above discussion, the continuous growing shear layer causes gradual accumulation of the circulation inside the toroidal vortex until it reaches a threshold denoted by C. The typical value of $C = 4$ for an ideal starting vortex jet (Gharib *et al.* 1998) is adopted here, although it could change notably under various conditions (Dabiri & Gharib 2005; Krueger *et al.* 2006; Lawson & Dawson 2013; Xia & Mohseni 2015). Applying $\Gamma_{TV}^* = C$ to (3.9) and solving for τ yields

$$f = \frac{1}{\tau} = \frac{1}{2C}\sqrt{\frac{g}{D}}\left(C_j Fr + \sqrt{C_j^2 Fr^2 + 2CC_h(r^* - 1)}\right). \tag{4.1}$$

This completes the derivation of the frequency relation for buoyancy-driven diffusion flames. (4.1) is similar to the scaling formula given by Eq. 1 of Cetegen & Ahmed (1993), with different power on the Fr term. An extended discussion on the differences of the two formulas will be provided at the end of this section. Now, let $Fr \to 0$, (4.1) can be further simplified to

$$f = \sqrt{\frac{C_h(r^* - 1)}{2C} \cdot \frac{g}{D}}, \tag{4.2}$$

which recovers the prominent scaling law, $f \propto (g/D)^{1/2}$, obtained by Byram & Nelson (1970), among others.

Next, we compare the theoretical formula with experiment for validation. Figure 4(a) shows the relation of f against $\sqrt{g/D}$ for various pool flames and jet flames from existing literature, which have diverse fuel types, fire source dimensions, and gravities. The experimental data are in good agreement with (4.2), and confirms the unification of the theory for buoyant diffusion flames. Similar comparisons of data were reported by Hamins *et al.* (1992) and Cetegen & Ahmed (1993) to demonstrate the relation of $f \sim \sqrt{D}$. However, we further verified the relation of $f \sim \sqrt{g/D}$ with the pool flames of varying gravity between $0.5g$ and $1.0g$ (Yoshihara *et al.* 2013) and the jet flames of varying gravity between $1.5g$ and $6.0g$ (Durox *et al.* 1995). The trend line obtained from figure 4(a), $f = 0.48\sqrt{g/D}$ with g being 9.8 m/s^2, is equivalent to the scaling relation, $f = 1.5\sqrt{1/D}$, given by Cetegen & Ahmed (1993). This suggests that the relation,

$$\sqrt{\frac{C_h(r^* - 1)}{2C}} = 0.48, \tag{4.3}$$

applies to all buoyant diffusion flames. Consequently, we can use (4.3) to eliminate the undetermined prefactor C_h and rewrite (4.1) as

$$St = \frac{C_j}{2C}\sqrt{Fr} + \sqrt{\left(\frac{C_j}{2C}\right)^2 Fr + \frac{1}{4.34Fr}}, \tag{4.4}$$

(a)

(b)
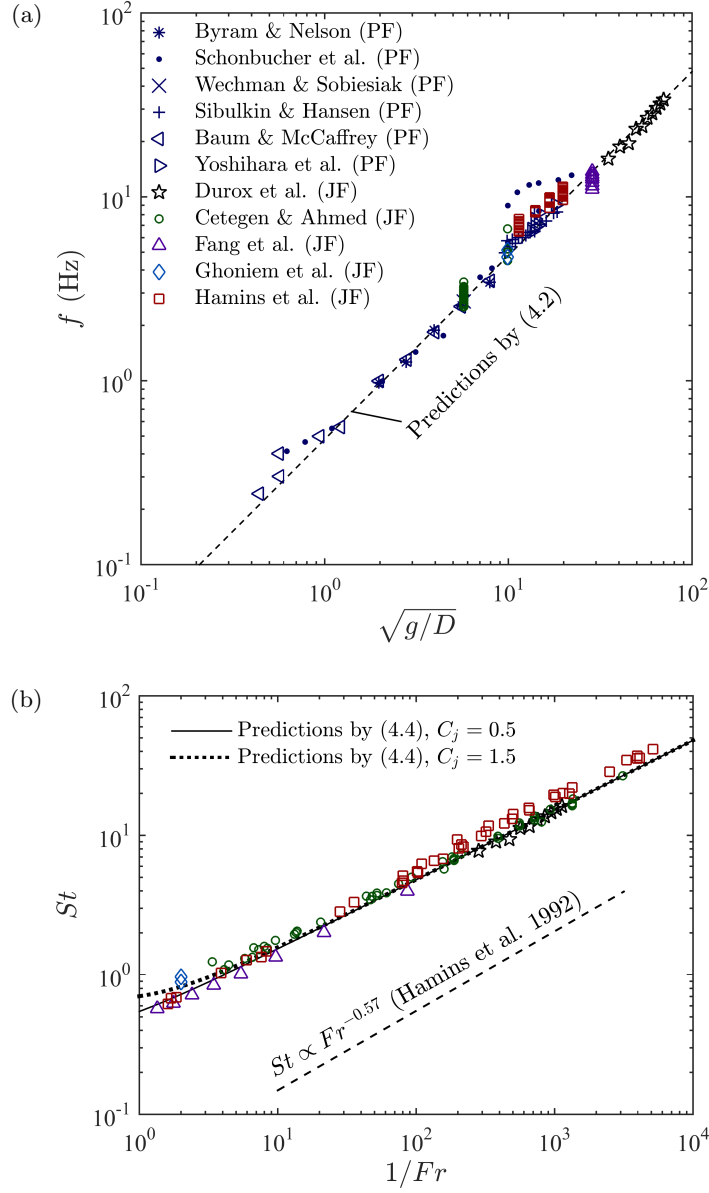
FIGURE 4. (a) Flickering frequencies (f) of pool and jet flames as a function of $\sqrt{g/D}$, with data collected from Byram & Nelson (1970); Sibulkin & Hansen (1975); Schönbucher *et al.* (1988); Baum & McCaffrey (1989); Weckman & Sobiesiak (1989); Hamins *et al.* (1992); Cetegen & Ahmed (1993); Durox *et al.* (1995); Ghoniem *et al.* (1996); Yoshihara *et al.* (2013); Fang *et al.* (2016). The gravitational acceleration was adjusted in the range of $1.5g \sim 6.0g$ for Durox *et al.* (1995)'s jet flames, and $0.5g \sim 1.0g$ for Yoshihara *et al.* (2013)'s pool flames. 'PF' and 'JF' in the legend represent pool flame and jet flame, respectively. (b) Theoretical predictions of St vs. $1/Fr$ for all jet flames in (a).

where the Strouhal number is defined as $St = fD/U_0$. We arrived at the non-dimensional frequency formula of flame flickering, where the only undetermined scaling factor is C_j, related to the boundary condition of the fuel inlet.

Figure 4(b) plots the experimental data from all jet flames in figure 4(a), showing
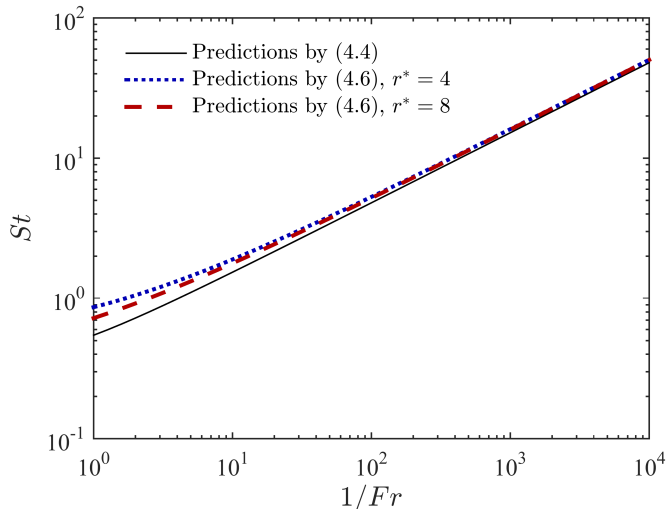
FIGURE 5. Comparison between the current theory (4.4) with $C_j = 0.5$ and Cetegen & Ahmed (1993)'s model (4.6). r^* for a common diffusion flame varies between 4 and 8.

generally promising agreement with the predictions by (4.4). It is seen that the theoretical predictions with $C_j = 0.5$ and $C_j = 1.5$ are almost identical for $Fr < 0.1$, and $C_j = 0.5$ shows a better agreement with the experimental data for $Fr > 0.1$. This is beyond the range of $Fr \ll 1$, based on which the present theory is derived. The result does suggest that the applicable range of this theory can be extended to $Fr \leqslant 1$. Equation (4.4) should also be valid for pool flames; however, since U_0 for those pool flames in figure 4(a) were not measured or reported, a direct validation is not available here. As a reference, we also plot the scaling relation of Hamins *et al.* (1992), which was obtained based on fitting jet flame data in the range of $10^{-6} < Fr < 10^8$. It is seen that their fitting line, with an exponent of -0.57, does not yield the best match with data in the $Fr < 1$ region, whereas the current theory (4.4) predicts that in the limit $Fr \to 0$ the exponent of the scaling law should be exactly -0.5.

Finally, we contrast our theory (4.4) with Eq. (1) of Cetegen & Ahmed (1993). Their equation was derived by applying the Bernoulli equation to calculate the convective velocity of the flame puff, which was then integrated to obtain the period as a function of the flame puff height, H_f, in the form of (Eq. (A12) of Cetegen & Ahmed (1993))

$$\tau^* = \frac{1}{St} = \frac{1}{C_f Ri} \left(\sqrt{\frac{2Ri H_f}{D} + 1} - 1 \right), \tag{4.5}$$

where C_f is a constant prefactor. It should be noted that Cetegen and Ahmed made two key assumptions. The first is a linear correlation between the inner flame velocity and the convective velocity of the flame puff, which was loosely implied from their previous work (Zukoski *et al.* 1985). The second is an implicit assumption that $H_f = D/2$, which removes possible dependence of the height of the flame puff on the dynamics of the toroidal vortex. So far, this assumption has not been supported by the existing literature. The current theory does not require these assumptions. For quantitative comparison, we rewrite Eq. (1) of Cetegen & Ahmed (1993) in the $St - Fr$ form,

$$St = K \left(\frac{1}{\sqrt{r^* - 1}} + \sqrt{\frac{1}{r^* - 1} + \frac{1}{Fr}} \right), \tag{4.6}$$

where the fitting parameter K was suggested by Cetegen and Ahmed to be 0.5 based on their experimental data. As seen in figure 5, both theories recover the same scaling law of $St \sim Fr^{-0.5}$ in the limit $Fr \to 0$. It is noted that (4.6) is explicitly dependent on r^*, which varies in a wide range for diffusion flames. This might explain why Cetegen & Ahmed (1993)'s formula predicted different K values for different jet flames as shown in their Fig. 14. In contrast, the present theory (4.4) is a unified one for buoyancy-driven jet flames, and relies on two physical constants C and C_j, the former accounting for the toroidal vortex detachment and the latter for the initial circulation of inflow.

5. Conclusions

The classic problem of flickering laminar diffusion flames was theoretically revisited in this study by performing vortex dynamics analysis. Considering the previous experimental observations that the flame flickering is synchronized with the periodic toroidal vortices, we sought further mathematical modelling to bridge the gap between the prominent frequency scaling and the dynamics of the toroidal vortices. By calculating the growth and detachment of a toroidal vortex, both of which are essential contributions to the periodicity of the flow field, we analytically derived a general formula which rigorously correlates the dynamics of the toroidal vortices with flame flickering. This presents a complete physical picture by incorporating the physically defined parameters C_j, C_h, and C that account for the vortex growth from the initial jet, the height correction of the toroidal vortex, and the detachment of the toroidal vortex, respectively. The formula shows convincing agreement with data from existing literature, especially for pool flames and jet diffusion flames with small Froude number.

The theory have profound significances in understanding the flickering of buoyant diffusion flames. One is the theoretical connection between the toroidal vortex mechanism and the prominent frequency scaling law. The other is a unified approach in treating pool flames and jet diffusion flames, regardless of the differences in fuel and burner. Specifically, we have shown that pool and jet flames share the same frequency formula at $Fr \to 0$, which does not depend on the initial fuel velocity U_0. This provides a theoretical support to the finding of Durox *et al.* (1995) and Sato *et al.* (2000) that the frequency is relatively independent of fuel velocity for a low-velocity jet flame, where buoyancy dominates over the initial jet flow. The future development of the current theory of buoyant diffusion flames can involve other mechanisms to capture the frequencies of jet diffusion flames with large Froude number, when gravitational effect becomes secondary.

6. Acknowledgements

REFERENCES

ALBERS, B. W. & AGRAWAL, A. K. 1999 Schlieren analysis of an oscillating gas-jet diffusion flame. *Combust. Flame* **119** (1-2), 84–94.

BATCHELOR, G.K. 1967 *An Introduction to Fluid Mechanics*. Cambridge: Cambridge University Press.

BAUM, H. R. & MCCAFFREY, B. J. 1989 Fire induced flow field-theory and experiment. *Fire Saf. Sci.* **2**, 129–148.

BEJAN, A. 1991 Predicting the pool fire vortex shedding frequency. *J. Heat Transfer (Transcations of the ASME, Series C)* **113** (1), 261–263.

BUCKMASTER, J. & PETERS, N. 1988 The infinite candle and its stabilitya paradigm for flickering diffusion flames. *Symp. Int. Combust. Proc.* **21** (1), 1829–1836.

BURKE, S. P. & SCHUMANN, T. E. W. 1928 Diffusion flames. *Ind. Eng. Chem.* **20** (10), 998–1004.

BYRAM, G. M. & NELSON, R. M. 1970 The modeling of pulsating fires. *Fire Tech.* **6** (2), 102–110.

CANTWELL, B., LEWIS, G. & CHEN, J. 1989 Topology of three-dimensional, variable density flows. In *10th Australasian Fluid Mechanics Conference*. Melbourne, Australia.

CARPIO, J., SÁNCHEZ-SANZ, M. & FERNÁNDEZ-TARRAZO, E. 2012 Pinch-off in forced and non-forced, buoyant laminar jet diffusion flames. *Combust. Flame* **159** (1), 161–169.

CETEGEN, B. M. 1997 Behavior of naturally unstable and periodically forced axisymmetric buoyant plumes of helium and heliumair mixtures. *Phys. Fluids* **9** (12), 3742–3752.

CETEGEN, B. M. & AHMED, T. A. 1993 Experiments on the periodic instability of buoyant plumes and pool fires. *Combust. Flame* **93** (1-2), 157–184.

CHAMBERLIN, D. S. & ROSE, A. 1948 The flicker of luminous flames. *Symp. Int. Combust. Proc.* **1**, 27–32.

CHEN, L. D. & ROQUEMORE, W. M. 1986 Visualization of jet flames. *Combust. Flame* **66** (1), 81–86.

CHEN, L. D., SEABA, J. P., ROQUEMORE, W. M. & GOSS, L. P. 1989 Buoyant diffusion flames. *Symp. Int. Combust. Proc.* **22** (1), 677–684.

COATS, C. M. 1996 Coherent structures in combustion. *Prog. Energy Combust. Sci.* **22** (5), 427–509.

COX, G. 1995 *Combustion fundamentals of fire*. Academic Press.

DABIRI, J. O. & GHARIB, M. 2005 Starting flow through nozzles with temporally variable exit diameter. *J. Fluid Mech.* **538**, 111–136.

DAVIS, R. W., MOORE, E. F., SANTORO, R. J. & NESS, J. R. 1990 Isolation of buoyancy effects in jet diffusion flame experiments. *Combust. Sci. Tech.* **73** (4-6), 625–635.

DETRICHE, P. H. & LANORE, J. C. 1980 An acoustic study of pulsation characteristics of fires. *Fire Tech.* **16** (3), 204–211.

DIDDEN, N. 1979 On the formation of vortex rings: Rolling-up and production of circulation. *Zeitschrift für Angewandte Mathematik und Physik* **30** (1), 101–116.

DUROX, D., YUAN, T., BAILLOT, F. & MOST, J. M. 1995 Premixed and diffusion flames in a centrifuge. *Combust. Flame* **102** (4), 501–511.

FANG, J., WANG, J.-W., GUAN, J.-F., ZHANG, Y.-M. & WANG, J.-J. 2016 Momentum- and buoyancy-driven laminar methane diffusion flame shapes and radiation characteristics at sub-atmospheric pressures. *Fuel* **163**, 295–303.

GHARIB, M., RAMBOD, E. & SHARIFF, K. 1998 A universal time scale for vortex ring formation. *J. Fluid Mech.* **360**, 121–140.

GHONIEM, A. F., LAKKIS, I. & SOTERIOU, M. 1996 Numerical simulation of the dynamics of large fire plumes and the phenomenon of puffing. *Symp. Int. Combust. Proc.* **26** (1), 1531–1539.

GLEZER, A. 1988 The formation of vortex rings. *Phys. Fluids* **31** (12), 3532–3542.

HAMINS, A., YANG, J. C. & KASHIWAGI, T. 1992 An experimental investigation of the pulsation frequency of flames. *Symp. Int. Combust. Proc.* **24** (1), 1695–1702.

JIANG, X. & LUO, K. H. 2000 Combustion-induced buoyancy effects of an axisymmetric reactive plume. *Proc. Combust. Inst.* **28** (2), 1989–1995.

JOULAIN, P. 1998 The behavior of pool fires: state of the art and new insights. *Symp. Int. Combust. Proc.* **27** (2), 2691–2706.

KATTA, V. R., GOSS, L. P. & ROQUEMORE, W. M. 1994 Numerical investigations of transitional H2/N2 jet diffusion flames. *AIAA Journal* **32** (1), 84–94.

KATTA, V. R. & ROQUEMORE, W. M. 1993 Role of inner and outer structures in transitional jet diffusion flame. *Combust. Flame* **92** (3), 274–282.

KLIMENKO, A. Y. & WILLIAMS, F. A. 2013 On the flame length in firewhirls with strong vorticity. *Combust. Flame* **160**, 335–339.

KOLHE, P. S. & AGRAWAL, A. K. 2007 Role of buoyancy on instabilities and structure of transitional gas jet diffusion flames. *Flow Turbul. Combust.* **79** (4), 343–360.

KRIEG, M. & MOHSENI, K. 2013 Modelling circulation, impulse, and kinetic energy of starting jets with non-zero radial velocity. *J. Fluid Mech.* **719**, 488–526.

KRUEGER, P., DABIRI, J. & GHARIB, M. 2006 The formation number of vortex rings formed in a uniform background co-flow. *J. Fluid Mech.* **556**, 147–166.

LAWSON, J. M. & DAWSON, J. R. 2013 The formation of turbulent vortex rings by synthetic jets. *Phys. Fluids* **25** (10), 105113.

LIÑÁN, VERA, M. & SÁNCHEZ, A. L. 2015 Ignition, liftoff, and extinction of gaseous diffusion flames. *Annu. Rev. Fluid Mech.* **47**, 293–314.

LIÑÁN, A., FERNÁNDEZ-TARRAZO, E., VERA, M. & SÁNCHEZ, A. L. 2005 Lifted laminar jet diffusion flames. *Combust. Sci. Tech.* **177** (5-6), 933–953.

LINGENS, A., NEEMANN, K., MEYER, J. & SCHREIBER, M. 1996 Instability of diffusion flames. *Symp. Int. Combust. Proc.* **26** (1), 1053–1061.

MALALASEKERA, W. M. G., VERSTEEG, H. K. & GILCHRIST, K. 1996 A review of research and an experimental study on the pulsation of buoyant diffusion flames and pool fires. *Fire Mater.* **20** (6), 261–271.

MAXWORTHY, T. 1972 The structure and stability of vortex rings. *J. Fluid Mech.* **51** (1), 15–32.

MAXWORTHY, T. 1977 Some experimental studies of vortex rings. *J. Fluid Mech.* **81** (3), 465–495.

MAXWORTHY, T. 1999 The flickering candle: transition to a global oscillation in a thermal plume. *J. Fluid Mech.* **390**, 297–323.

McCAMY, C. S. 1956 A five-band recording spectroradiometer. *J. Res. Natl. Bur. Stand.* **56** (5), 293.

MELL, W. E., McGRATTAN, K. B. & BAUM, H. R. 1996 Numerical simulation of combustion in fire plumes. *Symp. Int. Combust. Proc.* **26** (1), 1523–1530.

MOHSENI, K. & GHARIB, M. 1998 A model for universal time scale of vortex ring formation. *Phys. Fluids* **10** (10), 2436–2438.

NITSCHE, M. & KRASNY, R. 1994 A numerical study of vortex ring formation at the edge of a circular tube. *J. Fluid Mech.* **276**, 139–161.

PORTSCHT, R. 1975 Studies on characteristic fluctuations of the flame radiation emitted by fires. *Combust. Sci. Tech.* **10** (1-2), 73–84.

ROQUEMORE, W. M., CHEN, L. D., SEABA, J. P., TSCHEN, P. S., GOSS, L. P. & TRUMP, D. D. 1987 Jet diffusion flame transition to turbulence. *Phys. Fluids* **30** (9), 2600.

SAFFMAN, P. G. 1978 The number of waves on unstable vortex rings. *J. Fluid Mech.* **84** (4), 625–639.

SATO, H., AMAGAI, K. & ARAI, M. 2000 Diffusion flames and their flickering motions related with Froude numbers under various gravity levels. *Combust. Flame* **123** (1-2), 107–118.

SCHÖNBUCHER, A., ARNOLD, B., BANHARDT, V., BIELLER, V., KASPER, H., KAUFMANN, M., LUCAS, R. & SCHIESS, N. 1988 Simultaneous observation of organized density structures and the visible field in pool fires. *Symp. Int. Combust. Proc.* **21** (1), 83–92.

SHARIFF, K. & LEONARD, A. 1992 Vortex rings. *Ann. Rev. Fluid Mech.* **24** (1), 235–279.

SIBULKIN, M. & HANSEN, A. G. 1975 Experimental study of flame spreading over a horizontal fuel surface. *Combust. Sci. Tech.* **10** (1-2), 85–92.

TIESZEN, S. R. 2001 On the fluid mechanics of fires. *Annu. Rev. Fluid Mech.* **33** (1), 67–92.

TIESZEN, S. R., NICOLETTE, V. F., GRITZO, L. A., MOYA, J., HOLEN, J. & MURRAY, D. 1996 Vortical structures in pool fires: Observation, speculation, and simulation. *Tech. Rep.* No. SAND-96-2607. Sandia National Labs., Albuquerque, NM (USA).

TREFETHEN, L. M. & PANTON, R. L. 1990 Some unanswered questions in fluid mechanics. *Appl. Mech. Rev.* **43** (8), 153–170.

WECKMAN, E. J. & SOBIESIAK, A. 1989 The oscillatory behaviour of medium-scale pool fires. *Symp. Int. Combust. Proc.* **22** (1), 1299–1310.

WU, J. Z., MA, H. Y. & ZHOU, M. D. 2007 *Vorticity and Vortex Dynamics*. Springer.

XIA, X. & MOHSENI, K. 2015 Far-field momentum flux of high-frequency axisymmetric synthetic jets. *Phys. Fluids* **27** (11), 115101.

YOSHIHARA, N., ITO, A. & TORIKAI, H. 2013 Flame characteristics of small-scale pool fires under low gravity environments. *Proc. Combust. Inst.* **34** (2), 2599–2606.

YU, D. & ZHANG, P. 2017*a* On flame height of circulation-controlled firewhirls with variable physical properties and in power-law vortices: A mass-diffusivity-ratio model correction. *Combust. Flame* **182**, 36–47.

YU, D. & ZHANG, P. 2017*b* On the flame height of circulation-controlled firewhirls with variable density. *Proc. Combust. Inst.* **36** (2), 3097–3104.

ZHU, X., XIA, X. & ZHANG, P. 2018 Near-field flow stability of buoyant methane/air inverse diffusion flames. *Combust. Flame* **191**, 66–75.

ZUKOSKI, E. E., CETEGEN, B. M. & KUBOTA, T. 1985 Visible structure of buoyant diffusion flames. *Symp. Int. Combust. Proc.* **20** (1), 361–366.